



Contents lists available at ScienceDirect

Earth and Planetary Science Letters

www.elsevier.com/locate/epsl



Geophysical constraints on the water content of the lunar mantle and its implications for the origin of the Moon

Shun-ichiro Karato¹

Yale University, Department of Geology and Geophysics, New Haven, CT 06520, USA

ARTICLE INFO

Article history:

Received 25 February 2013

Received in revised form 30 September 2013

Accepted 2 October 2013

Available online 1 November 2013

Editor: C. Sotin

Keywords:

the Moon

water

tidal dissipation

electrical conductivity

giant impact

ABSTRACT

Although the Moon was considered to be “dry”, recent measurements of hydrogen content in some of the lunar samples showed a substantial amount of water comparable to the water content in the Earth's asthenosphere. However, the interpretation of these observations in terms of the distribution of water in the lunar interior is difficult because the composition of these rocks reflects a complicated history involving melting and crystallization. In this study, I analyze geophysically inferred properties to obtain constraints on the distribution of water (and temperature) in the lunar interior. The electrical conductivity inferred from electromagnetic induction observations and the geodetically or geophysically inferred Q are interpreted in terms of laboratory data and the theoretical models on the influence of water (hydrogen) on these properties. Both electrical conductivity and Q are controlled by defect-related processes that are sensitive to the water (hydrogen) content and temperature but less sensitive to the major element chemistry. After a correction for the influence of the major element chemistry constrained by geophysical observations and geochemical considerations, I estimate the temperature–water content combinations that are consistent with the geophysically inferred electrical conductivity and Q . I conclude that the lunar interior is cooler than Earth (at the same depth) but the water content of the lunar mantle is similar to that of Earth's asthenosphere. A possible model is presented to explain the not-so-dry Moon where a small degree of water loss during the Moon formation is attributed to the role of liquid phases that play an important role in the Moon-forming environment.

© 2013 Elsevier B.V. All rights reserved.

1. Introduction

The Moon and Earth share similar chemical compositions including some isotopic compositions, yet these planetary bodies show marked difference in the composition of the volatile and siderophile (iron-loving) elements (Ringwood, 1979; Wiechert et al., 2001; Wiczorek et al., 2006; Zhang et al., 2012). The Moon is significantly more depleted (relative to Earth) in most volatile (defined by their condensation temperatures) and siderophile elements. The similarities and differences in chemical compositions of these planetary bodies carry crucial information on the origin of the Moon. Ringwood (1979), for example, developed a model of the origin of the Moon where a large fraction of materials of the Moon was from Earth's mantle after the separation of the core. The depletion in volatile elements in this type of model is attributed to the volatile loss associated with high temperatures caused by a giant impact (e.g., Canup, 2004b; Ringwood, 1979; Wiczorek et al., 2006).

However, recent geochemical studies of some of the lunar samples present a challenge to a conventional view of highly de-

pleted and “dry” Moon (Boyce et al., 2010; Greenwood et al., 2011; Hauri et al., 2011; Saal et al., 2008). According to these studies, the interior of the Moon may contain as much water (and other volatile elements) as the Earth's asthenosphere (~0.01 wt% of water, Hirschmann, 2006). This is a remarkable observation because the concentration of volatile elements usually follows their condensation temperatures, and if the condensation temperature were used as a guide, then one would expect much smaller concentration of water (hydrogen) in the Moon (e.g., Ringwood, 1979).

However, the significance of these geochemical observations on the water content in the deep lunar mantle is unclear because the link between the composition of mantle materials and that of samples collected at the surface is not always simple. For instance, Elkins-Tanton and Grove (2011) presented a model to explain the influence of magma ocean evolution on the distribution of water assuming initially “damp” magma ocean (0.01 and 0.1 wt% of water). This model predicts a layered water content, relatively water-poor shallow mantle and water-rich deep mantle, but there have been no observational constraints on the water distribution in the deep lunar mantle. In fact, these authors prefer a model with small total water content in the shallow mantle to explain the composition of KREEP (lunar samples rich in incompatible elements). How-

E-mail address: shun-ichiro.karato@yale.edu.

¹ Tel.: +1 203 432 3147; fax: +1 203 432 3134.

Table 1

Parameters for electrical conductivity in Eq. (2). Data are from Karato and Wang (2013) numbers in the parenthesis are the errors. Parameters are for Mg# = 83. The reference values are $f_{O_2,0}$: Fe–FeO buffer, $C_{W0} = 0.01$ wt%.

	A_d (S/m)	A_w (S/m)	H_d^* (kJ/mol)	H_w^* (kJ/mol)	r_σ	q_d	q_w
olivine	$10^{2.3(0.2)}$	$10^{1.7(0.4)}$	154 (5)	87 (5)	0.62 (0.02)	0.17 (0.05)	-0.1^{\S}
opx	$10^{2.4(0.2)}$	$10^{1.3(0.3)}$	147 (6)	82 (3)	0.62^{\S}	0.17 (0.05)	$-0.1^{\S\S}$

[§] A value taken from the results for wadsleyite (Dai and Karato, 2009c).

^{§§} Assumed to be the same as olivine (Dai and Karato, 2009a).

ever, the reason for a relatively large amount of initial water content of the lunar magma ocean was not explained in their paper.

The purposes of this paper are (i) to interpret two geophysically inferred properties (electrical conductivity and tidal Q) to provide additional constraints on the distribution of water in the deep lunar interior and (ii) to discuss a possible explanation of relatively large water content of the Moon assuming a giant impact origin of the Moon.

2. Geophysical constraints on the distribution of water in the Moon

In addition to the measurements of compositions of rock samples, geophysical remote sensing can also provide important constraints on the water content in a terrestrial planet (Karato, 2006). Geophysically inferred properties that we use must be sensitive to water content and the sensitivity to other parameters must be small or well characterized. In most cases, properties that are sensitive to water content involve thermally activated processes and hence they are also sensitive to temperature (in general these properties are also dependent on pressure (P)). However, for electrical conductivity and anelasticity, the influence of pressure in the lunar mantle ($P < 4.5$ GPa) is small (for details see the later part)). The dependence of these properties (X) on various parameters may be symbolically written as,

$$X = X(C_W, T; \xi) \quad (1)$$

where C_W is water content, T is temperature, and ξ is composition other than water content (e.g., major element chemistry). In order to obtain useful constraints on water content, one needs to use properties for which the influence of “other” factors (ξ) is weak and/or can be evaluated with sufficient accuracy. In many cases, these properties are sensitive to both water content and temperature. In such a case, one can infer the combination of temperature and water content (C_W, T) that are consistent with geophysically inferred properties of the Moon. If we use two properties, then a combination of temperature and water content can be estimated uniquely within some uncertainties.

In the following, I will use the following strategy in using geophysical models. First, I will review the studies of major element chemistry (ξ in Eq. (1)) based on seismic wave velocities and gravity (+ geochemical observations). Seismic wave velocities and gravity are sensitive to the major element chemistry but insensitive to water content and only weakly sensitive to temperature (Karato, 2011). Consequently, the major element chemistry models inferred from such an approach (e.g., Khan et al., 2007; Kuskov and Kronrod, 1998) are relatively independent of water content (and temperature). These studies show that the models that are allowed by these geophysical observations are largely consistent with the results of geochemical/petrological studies (e.g., Ringwood, 1979; Wiczorek et al., 2006). In the following, I use a mineralogical model of the lunar mantle similar to the pyrolite model of the Earth's mantle with Mg# = 83 (Mg# is a molar ratio of Mg to (Mg + Fe) defined by $Mg\# = Mg/(Mg + Fe) \times 100$).

Regarding the depth variation in the major element chemistry, astronomically determined I/MR^2 (I : the moment of inertia, M :

total mass, R : radius) ($= 0.3931 \pm 0.0002$; Konopliv et al., 2001) provides a tight constraint on the degree of density (and hence compositional) stratification. This value implies a small depth dependence of density in the mantle. The depth variation in Mg#, for example, should be less than ~ 5 .

Then using the estimated range of ξ (e.g., major element chemistry), I will infer the combinations of water content and temperature that are consistent with the values of electrical conductivity and anelasticity (seismic wave attenuation and tidal Q) inferred from geophysical or astronomical observations (Garcia et al., 2011; Hood et al., 1982a; Nakamura and Koyama, 1982; Williams et al., 2001). Uncertainties in the estimated water content and temperature caused by the uncertainties in mineralogy and major element chemistry will be discussed later.

2.1. Electrical conductivity

Electrical conductivity provides a strong constraint on the distribution of water (hydrogen) because electrical conductivity is highly sensitive to water content but relatively insensitive to other factors (Karato, 2011; Karato and Wang, 2013). The use of electrical conductivity is particularly attractive because a good model of conductivity-depth profile is available for the Moon based on the analysis of electromagnetic induction (Hood et al., 1982a).

Electrical conductivity depends on water content, temperature, major element chemistry and oxygen fugacity. The experimental results can be adequately summarized by the following relationship,

$$\sigma(T, C_W; \xi) = \sigma_o(\xi) \cdot \left(\frac{C_W}{C_{W0}}\right)^{r_\sigma} \left(\frac{f_{O_2}}{f_{O_2,0}}\right)^q \times \exp\left(-\frac{H_\sigma^*}{R} \left(\frac{1}{T} - \frac{1}{T_o}\right)\right) \quad (2)$$

where $\sigma(T, C_W; \xi)$ is electrical conductivity, $\sigma_o(\xi)$ is the electrical conductivity at the reference water content, oxygen fugacity and temperature C_{W0} is the water content for the reference state (suffix “o” means the reference state), f_{O_2} is oxygen fugacity (this term could be included in $\sigma_o(\xi)$ but I treat this explicitly), r_σ is the water content exponent, q is the oxygen fugacity exponent, R is the gas constant, T is temperature and H_σ^* is the activation enthalpy for electrical conductivity. Influence of confining pressure (P) is generally weak, activation volume being ~ 1 cm³/mol or less (Dai and Karato, 2009b; Xu et al., 2000) and can be ignored for the Moon ($P < 4.5$ GPa). If several mechanisms of conduction operate, then contribution from each needs to be added, $\sigma = \sum_i \sigma_i$ where σ_i is electrical conductivity of the i -th mechanism (e.g., ferric iron (“polaron”) conduction + hydrogen conduction). The influence of the major element chemistry such as that of Mg# can be included through $\sigma_o = \sigma_o(\xi)$ to a good approximation (Hirsch and Shankland, 1993).

The parameters in the relationship (2) are summarized in Table 1 with the estimated experimental uncertainties. Somewhat different experimental results have been published on the influence of water (see e.g., Yoshino, 2010). Possible causes of differences are discussed by Karato (2013), Karato and Wang (2013). The

results from Yoshino's group would predict larger water content and higher temperature for a given conductivity, but the differences in inferred temperature and water content are not large compared to the uncertainties associated with this approach (for details, see Section 3). In this table, the experimental data for olivine and orthopyroxene are shown. Pyrope garnet will exist only in the deep mantle (below ~ 800 km). In the shallow mantle, other phases such as plagioclase or spinel will exist. But these minerals occupy only a small volume fraction ($\sim 10\%$), and their direct contribution is small. The most important role of these Al_2O_3 bearing minerals is to buffer the Al_2O_3 content in orthopyroxene.

Electrical conductivity is dependent on oxygen fugacity (either positive or negative dependence; e.g., Karato and Wang, 2013). Geochemical studies on lunar samples make a strong case for low f_{O_2} conditions (close to or below the Fe–FeO buffer) in the shallow portions of the Moon (Wieczorek et al., 2006). However, oxygen fugacity in the deep mantle could change with depth. Wieczorek et al. (2006) discussed a possibility that oxygen fugacity increases with depth reaching to the FMQ (fayalite–magnetite–quartz) buffer. However, Frost and McCammon (2008) presented evidence that oxygen fugacity in the Earth's upper mantle progressively decreases with depth relative to the FMQ buffer. Because of these uncertainties, I will consider both high f_{O_2} (FMQ buffer) and low f_{O_2} (Fe–FeO buffer) models.

Given the major element chemistry, mineralogy and oxygen fugacity, I calculate electrical conductivity of each mineral for assumed total water contents. I assume that the total water content and the major element chemistry such as Mg# are independent of depth. Then temperature needed to explain the inferred electrical conductivity is calculated as a function of depth for assumed total water content (later, I will also estimate a combination of temperature and water content that explain geophysically inferred conductivity).

In the following, I will calculate the temperature–depth profiles from the conductivity–depth profiles published by Hood et al. (1982a) for a range of water content. The electrical conductivity was inferred from the observed frequency dependence of the transfer function. Electrical conductivity is best resolved in the mid-mantle (~ 400 – 1200 km) where the uncertainty is a factor of $\sim \pm 2$ (Hood et al., 1982a).

Fig. 1 shows the results of such calculations. In order to see the influence of mineralogy, I considered two end-member models, pure olivine and pure orthopyroxene models. The temperatures predicted for a completely dry (water-free) model are substantially higher than the temperatures inferred from other methods (e.g., Khan et al., 2007; Kuskov and Kronrod, 1998; Lambeck and Pullan, 1980; Nimmo et al., 2012) and exceed the dry solidus below ~ 1000 km although the estimated temperatures depend on the assumed mineralogy and oxygen fugacity (Fig. 1). A large extent of partial melting can be ruled out by the seismological studies (Khan et al., 2007; Kuskov and Kronrod, 1998; Toksöz, 1974) (a small degree of partial melting just above the core is proposed by Weber et al., 2011, but this layer is so thin that it does not affect the main conclusion of this paper), and therefore I conclude that a completely dry model can be rejected. The water content of ~ 0.01 – 0.001 wt% provides a temperature–depth profile below the solidus and similar to the one inferred from other geophysical approaches (Khan et al., 2007; Kuskov and Kronrod, 1998; Lambeck and Pullan, 1980; Nimmo et al., 2012).

The uncertainties in the inferred temperature–depth profiles come from (i) the uncertainties in the conductivity–depth models, (ii) the uncertainties in the major element chemistry (i.e., a factor ξ), (iii) the uncertainties in oxygen fugacity and (iv) the uncertainties in the dependence of the electrical conductivity on water content and temperature for a given mineral. As shown in Table 1, the uncertainties in the mineral physics parameters are

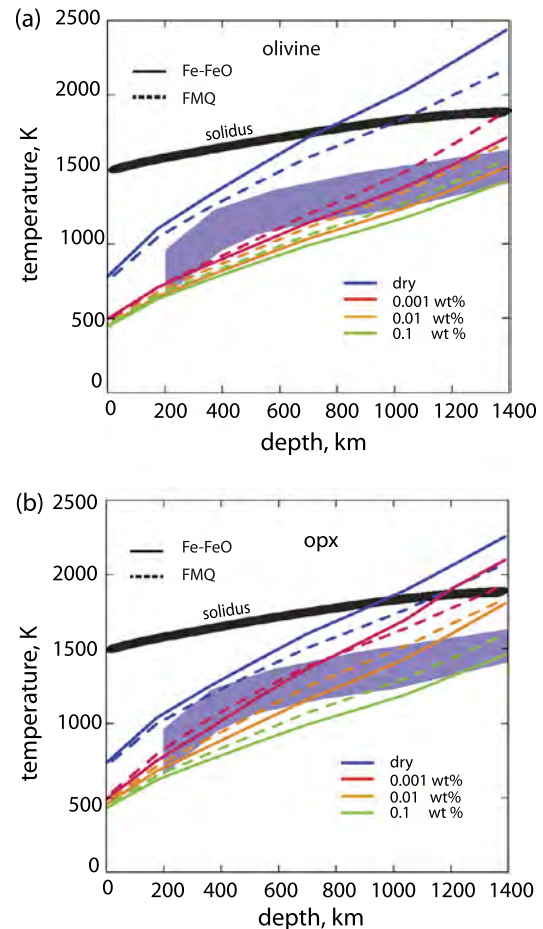


Fig. 1. Temperature–depth profiles of the Moon's interior inferred from electrical conductivity (Mg# = 83 and Al_2O_3 in orthopyroxene is 1 wt%). (a) olivine model, (b) orthopyroxene model. Solid curves are for f_{O_2} corresponding to the Fe–FeO buffer (at the surface) and broken curves to the FMQ buffer. f_{O_2} is assumed to be independent of depth (uncertainties in the depth dependence are within these two end-member cases). A thick black curve shows the solidus. For the water content inferred from this study (0.001–0.01 wt%), the influence of water on solidus is small (less than ~ 50 K reduction), although water effect is large (~ 200 K reduction) if water content is as high as 0.1 wt% (Hirschmann, 2006). The purple region shows a range of temperature for the lunar mantle estimated from other geophysical observations (e.g., Khan et al., 2007; Kuskov and Kronrod, 1998; Lambeck and Pullan, 1980). Forward model calculation on temperatures provide similar results with larger uncertainties (e.g., Nimmo et al., 2012). (For interpretation of the references to color in this figure, the reader is referred to the web version of this article.)

small. For example, the activation enthalpy has been determined to a high precision (better than 5%), and the uncertainty in the water content exponent r_σ is $\sim 10\%$ leading to the uncertainties in the inferred temperature of $\sim \pm 80$ K.

Potentially more important sources of uncertainties are those caused by the uncertainties in ξ (major element chemistry). Four issues are critical. (i) Mg#, (ii) Al_2O_3 content in orthopyroxene, (iii) olivine to orthopyroxene ratio, and (iv) f_{O_2} . Mg# is potentially important. A range of Mg# proposed for the Moon is Mg# = 82–88 (Kuskov and Kronrod, 1998) and the influence of Mg# in this range (85 ± 3) on the inferred temperature estimate is small ($\sim \pm 50$ K). However, if Mg# is as low as Mg# = 40 suggested by Elkins-Tanton et al. (2011)'s model (in the deep mantle), then electrical conductivity will be higher than a typical mantle by a factor of ~ 100 leading to the temperature change of ~ 600 K. However such a large radial variation of Mg# is inconsistent with the moment of inertia observations. A potentially important major element chemistry is Al_2O_3 content in orthopyroxene that has a large effect on

Table 2

Parameters for anelasticity corresponding to Eq. (3) (partly from Jackson and Faul, 2010, numbers in the parenthesis are errors) and for the reference state based on geochemical and geophysical studies (for details, see text).

Q_o	C_{W0} (wt%)	ω_o^{\ddagger} (Hz)	T_o (K)	$C_{Wtr}^{\S\S}$ (wt%)	α	r_Q^{\S}	H_Q^* (kJ/mol)
80 (10)	0.01 ($^{+0.01}_{-0.005}$)	10^{-2}	1550 (50)	3×10^{-5}	0.3 (0.05)	0.3–0.6	110 (12)

[‡] The choice of reference frequency has a large uncertainty. In Dziewonski and Anderson (1981), Q was determined assuming (incorrectly) that it is independent of frequency and the reference frequency of 1 Hz is provided. However, when Q of the asthenosphere is determined using surface waves, a typical frequency is $\sim 10^{-2}$ Hz (e.g., Yang et al., 2007).

^{§§} Estimated from Mei and Kohlstedt (2000a).

[§] The value of r_Q ($=\alpha r_\eta$) has not yet been determined precisely. However, r_η has been determined for creep ($r_\eta \sim 1.0$ – 1.2 for diffusion and dislocation creep in olivine, Karato and Jung, 2003; Mei and Kohlstedt, 2000a, 2000b). Since creep and Q are closely related (Karato and Spetzler, 1990; McCarthy et al., 2011), $r_Q \sim 0.3$ ($\alpha \sim 0.3$) is a preferred value for olivine. However, a higher value is reported for grain-growth in wadsleyite (Nishihara et al., 2006) ($r_\eta = 1.7$) and creep of garnet (Katayama and Karato, 2008) ($r_\eta = 2.4$).

electrical conductivity (Huebner et al., 1979). Based on thermodynamics of Al_2O_3 partitioning, I use the results of electrical conductivity of orthopyroxene with ~ 1 wt% Al_2O_3 (Table 1). In summary, when the contributions from errors in each term in Eq. (2) are added using the error propagation relation (e.g., Bevington and Robinson, 2003), the error in the estimated temperature is $\sim \pm 100$ K (the error in water content is a factor of ~ 3).

The results shown in Fig. 1 suggest that a completely dry model of the Moon is difficult to reconcile with the constraints on the mantle temperature from other observations. However, due to the trade-off between water content and temperature, it is difficult to draw more detailed conclusions about the water content from electrical conductivity alone.

2.2. Anelasticity (seismic wave attenuation and tidal dissipation)

Similar to electrical conductivity, anelastic properties of minerals are sensitive to water content (and temperature) and hence observations on these properties could provide constraints on water content (Karato, 2006). Anelasticity is usually measured by a non-dimensional parameter Q that is the inverse of a fraction of dissipated energy per unit cycle. Energy dissipation occurs through some time-dependent processes, and hence Q generally depends on frequency. Because Q is a non-dimensional quantity, the frequency dependence must come through a non-dimensional variable, $\omega\tau$ where ω is frequency and τ is the characteristic time of relaxation. If energy dissipation occurs by viscous deformation, then τ is the Maxwell time (e.g., McCarthy et al., 2011), $\tau = \tau_M = \frac{\eta(T, C_W; \xi)}{M}$ where η is viscosity and M is shear modulus (pressure effect is weak, see Section 3). Hence $Q^{-1}(T, C_W; \omega; \xi) = Q^{-1}[\omega \cdot \tau(T, C_W; \xi)]$.

Experimental studies on anelasticity have been carried out for minerals under high temperature conditions at a modest pressure (for a review see Jackson, 2009). In most cases, the results can be described by the power-law relationship, $Q^{-1} \propto \omega^{-\alpha}$ with $\alpha \approx 0.3$ (e.g., Jackson, 2009; Karato, 2008). Using the Maxwell-time scaling and an empirical relationship, $\eta = \eta_o(\xi) \cdot \left(\frac{C_W}{C_{W0}}\right)^{-r_\eta} \exp\left(\frac{H_\eta^*}{RT}\right)$, one has

$$\frac{Q^{-1}(C_W, T; \omega; \xi)}{Q_o^{-1}(C_{W0}, T_o; \omega_o; \xi)} = \left(\frac{\omega}{\omega_o}\right)^{-\alpha} \left(\frac{C_W}{C_{W0}}\right)^{r_Q} \times \exp\left(-\frac{H_Q^*}{R} \left(\frac{1}{T} - \frac{1}{T_o}\right)\right) \quad (3)$$

where C_{W0} is the water content in the reference state, r_η is the water content exponent for viscosity (~ 1.2 ; Karato, 2008; Karato and Jung, 2003), H_η^* is activation enthalpy for viscosity, $r_Q = \alpha r_\eta$ and $H_Q^* = \alpha H_\eta^*$ where I assumed that the influence of major element chemistry is through its effect on the factor, Q_o^{-1} (for dry conditions, $r_Q = 0$). Similar to electrical conductivity, if there are multiple mechanisms, then contribution from each to Q^{-1} needs

to be added as $Q^{-1} = \sum_i Q_i^{-1}$ where Q_i^{-1} is Q^{-1} by the i -th mechanism. For example, when contributions from dry and wet mechanisms is considered, one can modify the relation (3) to

$$\frac{Q^{-1}(T, C_W; \omega; \xi)}{Q_o^{-1}(T_o, C_{W0}; \omega_o; \xi)} = \frac{1 + \left(\frac{C_W}{C_{Wtr}}\right)^{r_Q}}{1 + \left(\frac{C_{W0}}{C_{Wtr}}\right)^{r_Q}} \cdot \left(\frac{\omega}{\omega_o}\right)^{-\alpha} \times \exp\left(-\frac{H_Q^*}{R} \left(\frac{1}{T} - \frac{1}{T_o}\right)\right) \quad (4)$$

where C_{Wtr} is the water content at which the contribution from wet mechanism is equal to that of dry mechanism.

Q_o^{-1} depends on defect density such as grain-size and dislocation density as well as major element chemistry (Karato and Spetzler, 1990). The relation (3) shows that in addition to major element chemistry and defect density, Q^{-1} depends on water content and temperature, similar to electrical conductivity and therefore inferred Q^{-1} can be used to infer the water content (and temperature).

For the materials in the lunar mantle, the only data set of anelasticity is for olivine (a data is available for olivine and pyroxene mixture, Sundberg and Cooper, 2010, but that study was made at room pressure where pyroxene is proto-enstatite (at high temperature), and the influence of cracking may affect the results). Therefore I use the experimental data on olivine (Aizawa et al., 2008; Farla et al., 2012; Jackson and Faul, 2010). The influence of orthopyroxene is difficult to evaluate, but a rough estimate can be made if one uses the Maxwell-time scaling. In such a case, the influence of orthopyroxene can be made based on the experimental data on the influence of orthopyroxene on viscosity (long-term deformation). A compilation of existing data shows that the addition of orthopyroxene to olivine has minor effects (Karato, 2008) and I conclude that the influence of orthopyroxene on anelasticity is not large, and use the experimental data on olivine. Also for a small range of Mg# inferred for the Moon, the influence of Mg# on Q is small (less than 15%, if one uses the Maxwell-time scaling is used; Zhao et al., 2009). Table 2 summarizes the experimental data on anelasticity of olivine.

The application of the data summarized in Table 2 to seismic Q and tidal Q is not straightforward. The data summarized in Table 2 were collected for fine-grained specimens at low pressure (200 MPa). Therefore, well-characterized experimental data on Q are available only for grain-size sensitive regime. However, preliminary studies showed that the contribution from dislocation mechanisms could be equal to or larger than that of grain-size sensitive mechanism under the mantle conditions (e.g., Farla et al., 2012; Jackson, 2009). Consequently, rather than using a grain-boundary model of Q and calculate Q for assumed grain-size (or dislocation density), I will use the seismologically determined Q ($= 80$; Dziewonski and Anderson, 1981; Yang et al., 2007) in the asthenosphere as an anchor value (Q_o) and calculate Q for other temperatures, frequencies and water contents using the temperature, frequency and water content dependence of Q . Essentially,

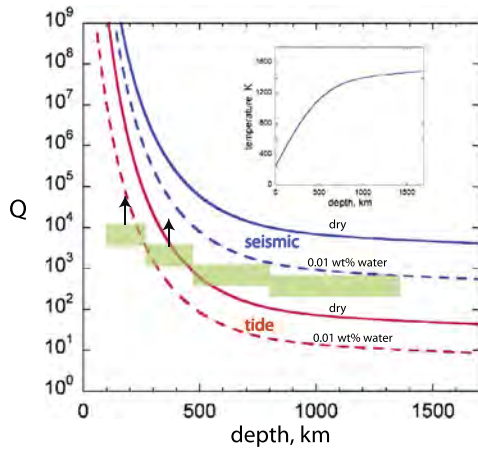


Fig. 2. Q versus depth relationships for various water content for seismic (1 Hz) and tidal frequency (10^{-6} Hz) corresponding to the temperature–depth relationship shown in the inset. Hatched regions correspond to Q determined seismologically (Garcia et al., 2011; Nakamura and Koyama, 1982). Seismologically determined Q corresponds to intrinsic Q as well as apparent Q caused by scattering. The frequency dependence of Q suggests that the influence of scattering is large (Nakamura and Koyama, 1982) (particularly in the shallow regions where intrinsic Q is large). In these cases, the Q values shown are the lower limits for the intrinsic Q (Q due to anelasticity).

I use Eq. (4) where Q_0^{-1} is a reference value ($= 1/80$), and calculate Q at different conditions using the relation (4). Because the values of frequency exponent and the activation enthalpy are similar between these two mechanisms, extrapolation from Q_0^{-1} does not involve large uncertainties caused by the uncertainties in the mechanisms of Q . Possible errors associated with the choice of reference state (anchor value) will be discussed later.

As can be seen from Eq. (3) (or (4)), the parameters that one needs in such calculations are α (frequency exponent), r_Q (water content exponent), and H_Q^* (activation enthalpy). Therefore the uncertainties associated with this calculation are caused by the uncertainties in these parameters (see Table 2), as well as the uncertainties in the reference state. Among them, the water content exponent (r_Q) is the least known parameter, but based on the scaling model, I choose $r_Q = 0.3$ (and 0.6) (corresponding to $r_\eta = 1-2$ ($r_\eta \approx 1$ for olivine, and therefore $r_Q \approx 0.3$ is a preferred value)). The uncertainties associated with this anchored value approach come partly from the assumed thermochemical conditions and frequency corresponding to the asthenospheric Q of Earth. Among them, temperature in the asthenosphere is $\sim 1550 \pm 50$ K (McKenzie and Bickle, 1988) and water content is 0.01 wt% (a factor of ~ 2 uncertainty) (Dixon et al., 2002; Hirschmann, 2006). The frequency at which $Q \sim 80$ is evaluated is ~ 0.01 Hz (Yang et al., 2007). Another source of uncertainties is the uncertainties in the implicitly assumed grain-size or dislocation density. This issue will be discussed later in Section 3.

Fig. 2 shows the calculated $Q(z)$ for both seismic (~ 1 Hz) and tidal ($\sim 10^{-6}$ Hz) frequency. The temperature–depth relations similar to the one by Khan et al. (2007) is used in this calculation (see the inset). The results for Q at seismic frequency may be compared with seismological observations (Garcia et al., 2011; Nakamura and Koyama, 1982; Nakamura et al., 1982). These observations show that the shallow lunar mantle has remarkably high seismic Q compared to Earth’s mantle, consistent with cold (and dry) interior. However, deep interior shows much lower Q (Garcia et al., 2011; Nakamura et al., 1982). Note, however, that seismic Q cannot be determined precisely when energy loss is small (large Q). When intrinsic energy loss due to anelasticity is small (high Q), inferred Q could come partly from scattering, and this leads to the underestimate of intrinsic Q (the frequency dependence of Q inferred by Nakamura and Koyama (1982) sug-

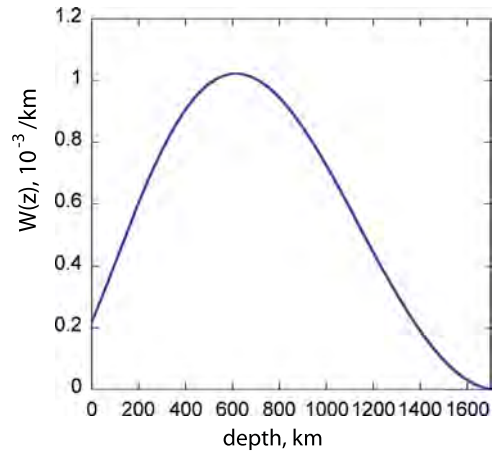


Fig. 3. The weighting function $W(z)$ for calculating tidal Q from the depth dependent Q . Tidal energy dissipation calculated by Peale and Cassen (1978) is used.

gests a contribution from scattering). Similarly, geometric focusing and defocussing effects can significantly affect the inferred Q . Consequently, seismic Q reported in these previous papers has large uncertainties particularly in shallow regions. Therefore seismologically determined Q values are used only as a guide, and the inference of water content and temperature will be made using tidal Q as constraints.

The tidal energy dissipation is the integrated energy dissipation of a planet, the relation between depth dependent Q and tidal Q is given by

$$Q_{\text{tide}}^{-1}(\omega_{\text{tide}}) = \int_0^R Q^{-1}(\omega_{\text{tide}}, r) \cdot W(r) \cdot dr \quad (5)$$

where $W(r)$ is a normalized weighting function ($\int_0^R W(r) \cdot dr = 1$) related to the distribution of tidal energy dissipation rate $\dot{E}(r)$ as $W(r) \cdot dr = 4\pi r^2 \dot{E}(r) \cdot dr$. The energy dissipation rate associated with tidal deformation of the Moon was calculated by Peale and Cassen (1978) and the weighting function calculated from this model is shown in Fig. 3. It is seen that the tidal dissipation is most sensitive to the energy dissipation in the middle mantle of the Moon.

Fig. 4 shows the results of calculated tidal Q as a function of water content where a range of tidal Q inferred from geodetic measurements is shown. Tidal Q is determined from the shape of the Moon (Williams et al., 2001) and consequently, the accuracy of tidal Q measurements is much better than that of seismic Q . For instance, Williams et al. (2001) reported estimated values of tidal energy dissipation through the analysis of the shape of the Moon yielding $Q = 40-60$ at monthly and annual period with the errors of $\pm 10-30\%$. The results show that the water content of ~ 0.01 wt% is consistent with the observed tidal Q but the dry model is not, a result consistent with the inference from electrical conductivity. However, the inferred water content depends on the assumed temperature, and is not unique. Later, I will combine Q and electrical conductivity observations together to evaluate the degree of trade-off between temperature and water content estimates.

The nominal uncertainties of tidal Q are $\pm 10-30\%$ (Williams et al., 2001) that correspond to the uncertainty in temperature of ± 60 K (for the activation enthalpy, H_Q^* , of ~ 110 kJ/mol and the frequency exponent (α) of ~ 0.3). The larger uncertainties come from the uncertainties in the anelastic properties of minerals and the uncertainties associated with the choice of an anchor value, Q_0 . One of the important sources of uncertainties is the validity of extrapolating the experimental results of grain-size sensitive

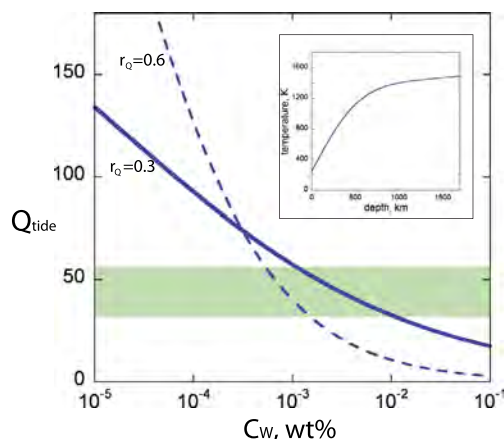


Fig. 4. Tidal Q versus water content. Tidal Q was calculated using $Q(z)$ profile for 10^{-6} Hz and taking the weighted average based on the strain energy versus depth profile for tidal deformation (Peale and Cassen, 1978). r_Q is the exponent representing the sensitivity of Q to water content ($Q \propto C_W^{-r_Q} \omega^\alpha$; C_W : water content, ω : frequency, $\alpha = 0.3$). In order to explain the observed tidal Q (40–60, shown by a green region), water content of ~ 0.01 – 0.001 wt% is required.

anelasticity to coarse grain-size in Earth and the Moon. There are two issues. One is that we do not know the grain-size in the lunar mantle with any confidence. Another uncertainty is the competition between grain-size sensitive and dislocation mechanisms of anelasticity.

To minimize the uncertainties, I used Q of Earth's asthenosphere as a reference Q (an anchored Q , Q_0) corresponding to the well-constrained temperature (pressure) and water content (e.g., Hirschmann, 2006; McKenzie and Bickle, 1988), and Q at different conditions were calculated relative to this reference value. Therefore the main factors that affect the conclusion are those used in calculating Q at temperature and water content that are different from those in the Earth's asthenosphere. These are the activation enthalpy and the water content exponent, r_Q . Among them the activation enthalpy is well known, but the water content exponent is poorly constrained. Therefore I used a range of water content exponent ($r_Q = 0.3$ – 0.6 ; Fig. 4) although $r_Q \sim 0.3$ is a preferred value if the Maxwell-time scaling is assumed.

The estimates of water content from either electrical conductivity or Q have large uncertainties if the estimate is made separately. In order to reduce the uncertainties, I now calculate the temperature and water content that are consistent with the geophysically inferred electrical conductivity and Q simultaneously. I chose the values of electrical conductivity and Q at 800 km depth (this depth is chosen because electrical conductivity is well constrained at that depth and the tidal Q is most sensitive to Q in the mid-mantle, Fig. 3). The results are shown in Fig. 5. The temperature of ~ 1200 – 1500 K and the water content of $\sim 10^{-3}$ – 10^{-2} wt% are consistent with these geophysically inferred properties. I conclude that the deep lunar mantle is cooler than Earth's mantle (compared at the same depth) but the water content is not much different from that of Earth's asthenosphere. The temperature in the mid lunar mantle inferred from this study is in good agreement with various thermal models (see a review by Nimmo et al., 2012) as well as the temperatures inferred from seismological as well as gravity measurements (Khan et al., 2007).

3. Discussion

3.1. Comparison to previous studies

In some previous studies where electrical conductivity of the lunar mantle was interpreted in terms of the temperature and composition, temperatures less than the solidus were inferred

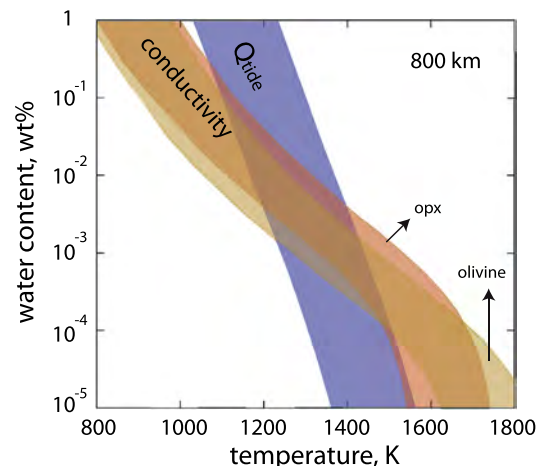


Fig. 5. Temperature–water content combinations (T, C_W) that are consistent with the inferred electrical conductivity and Q value at 800 km depth ($r_Q = 0.3$). For conductivity, the results for olivine and orthopyroxene are used to show the range of uncertainties caused by the mineralogy (results are for Fe–FeO buffer). Hatched regions show (T, C_W) combinations consistent with electrical conductivity and Q . If both electrical conductivity and Q need to be explained, the temperature–water content combination at this depth must be 1200–1500 K and 10^{-3} to 10^{-2} wt%.

without invoking the influence of water (Hood et al., 1982b; Huebner et al., 1979; Khan et al., 2006). The main cause for this difference is the different amount of Al_2O_3 assumed in these studies. An increase in Al_2O_3 content in orthopyroxene from 0.5 wt% to 5 wt% will increase electrical conductivity by a factor of ~ 10 (Huebner et al., 1979) leading to the reduction of inferred temperature by ~ 300 K. The bulk lunar mantle is estimated to have 4–5 wt% of Al_2O_3 (Khan et al., 2007; Ringwood, 1979; Wieczorek et al., 2006). Hood et al. (1982b), Huebner et al. (1979), Khan et al. (2006) considered that all Al_2O_3 is in orthopyroxene. However, this is inconsistent with the known thermodynamics of partitioning of Al_2O_3 among co-existing minerals. In the deep lunar mantle, a majority of Al_2O_3 should be in garnet (in shallow mantle other minerals such as plagioclase play a similar role), and the Al_2O_3 content in orthopyroxene should be less than ~ 1 wt% (based on the data by Perkins et al., 1981). Also a high Fe content in some thick layers of the lunar mantle can be ruled out from the observed moment of inertia. Grimm (2013) recently published a related work in which he revisited the electromagnetic induction observations (transfer function) including the effects of water. His analysis is focused on the electrical conductivity of the shallow mantle (shallower than 600 km) below the Procellarum KREEP Terrane where the chemistry of the surface rocks suggests anomalous lunar interior, whereas my analysis is on the globally averaged structure (and the deep mantle). In contrast to my analysis where the strong trade-off between temperature and water content is resolved by the joint analysis of electrical conductivity and tidal dissipation, Grimm uses thermal models to place constraints on the temperature. The thermal models in the shallow part are highly sensitive to the assumed amount of heat production and it is not easy to obtain a definitive conclusion on the water content.

The inferred temperature and water content from the present analysis would be somewhat different if the electrical conductivity model by Yoshino group were used. Essentially, Yoshino's group reports a factor of ~ 10 lower electrical conductivity than Karato's group compared at the same conditions. This would shift the T – C_W domain consistent with electrical conductivity and tidal dissipation observations to higher values (T to ~ 150 K and C_W to a factor of ~ 5 higher). Even using these data, we have a conclusion similar to the one with the data by Karato's group that the lunar interior is colder than Earth (at the same depth), but has the water content similar to Earth's upper mantle.

In many previous studies on the interpretation of seismic attenuation or tidal Q , Q was calculated for assumed grain-size and temperature-depth profile and the plausibility of these assumed values was discussed (e.g., [Faul and Jackson, 2005](#); [Nimmo et al., 2012](#)). However, such an approach is not quite satisfactory, because one can explain any values of Q assuming corresponding grain-size (or other defect density) and hence no constraint on water content will be obtained from such an approach. In addition, the sensitivity of Q to water content is not as strong as that of electrical conductivity as seen in [Fig. 5](#) and it is difficult to place constraints on water content from tidal Q alone. Also it is not clear if grain-size sensitive mechanism of anelasticity dominates or not. A crude estimate suggests that these two mechanisms could contribute nearly equally ([Farla et al., 2012](#); [Jackson, 2009](#)). If dislocation mechanism dominates, then the approach assuming grain-size sensitive mechanism will no longer be valid.

In addition, such an approach is subject to the large uncertainty caused by the unknown pressure effect (lab data are collected at 0.2 GPa, but the pressures in the lunar mantle goes to ~ 4.5 GPa). For a plausible value of activation volume of ~ 5 – 15 cm³/mol (e.g., [Karato, 2010](#)), the uncertainties in the pressure effect is to change Q (at 4 GPa) by a factor of 2–3 that is larger than the uncertainties caused by any other factors. Such an uncertainty is avoided in an anchored value approach used here where we start from ~ 4 GPa and the majority of contribution to tidal Q comes from deep interior.

In both [Nimmo et al. \(2012\)](#) and my model, seismic Q is over-estimated compared to the reported values. As I discussed before, this discrepancy is likely caused by the difficulties in estimating the intrinsic Q from seismology when Q is large (intrinsic Q is likely under-estimated from seismological observations in the shallow mantle).

3.2. Uncertainties associated with the anchor Q value (Q_0)

The use of an anchored value of Q eliminates some of the arbitrariness or the uncertainties inherent to the interpretation of Q . In this approach, one of the uncertainties comes from the possible difference in Q value between the Earth's asthenosphere and the lunar mantle at the same temperature and water content. Because parameters such as frequency, temperature and water content are factored out when I define Q_0 , and because the major element chemistry has only small influence on Q , the uncertainties associated with Q_0 are essentially the uncertainties on the relevant defect density (e.g., grain-size, dislocation density). The defect density relevant to Q is likely the defect density at the time of last deformation event (including the on-going deformation; e.g., [Karato, 1984](#)).

Let us consider a case of grain-size sensitive anelasticity. In this case, Q depends on grain-size (d) as $Q_0^{-1} \propto d^{-\beta}$ with $\beta \approx 0.25$ ([Jackson and Faul, 2010](#)). Now grain-size during deformation is controlled by stress (σ) through dynamic recrystallization as $d \propto \sigma^{-\zeta}$ with $\zeta \approx 1.2$ ([Karato et al., 1980](#)). So $Q_0^{-1} \propto \sigma^{\beta\zeta} \approx \sigma^{0.3}$. A similar relation will hold for dislocation mechanism (e.g., [Karato, 1998](#)) although detailed studies have not been made on it. Given these relationship, the essential question is how similar is the stress between Earth and the Moon at the same temperature and water content. Using a standard theory of convection, stress during thermal convection is given by (e.g., [Schubert et al., 2001](#)) $\sigma \approx \frac{\eta\kappa}{l^2} Ra^{2/3} = (\eta\kappa)^{1/3} (\Delta T \cdot \rho\alpha g)^{2/3}$ where η is viscosity, ΔT is temperature difference between the surface and the interior, κ is thermal diffusivity, ρ is density, α is thermal expansion, and g is acceleration due to gravity. Among various factors, $\eta\kappa$ depends essentially on temperature and water content and hence should be the same between the Moon and Earth at the same temper-

ature and water content, and the temperature difference is also similar if one uses the potential temperature as temperature inside of a planet. Therefore Q in the Moon and in Earth at the same temperature and water content is related as $\frac{Q_0^{-1}(\text{Moon})}{Q_0^{-1}(\text{Earth})} = \left(\frac{\rho(M)}{\rho(E)} \frac{\alpha(M)}{\alpha(E)} \frac{g(M)}{g(E)}\right)^{2/3} \beta\zeta \sim 0.7$. Applying the error propagation analysis including all sources of uncertainties ([Bevington and Robinson, 2003](#)), I estimate that the errors in estimated temperature from Q is ± 100 K (errors in water content of a factor of ~ 3 – 5).

3.3. Partial melting?

High conductivity and low Q (and low seismic wave velocities) are often attributed to partial melting (e.g., [Shankland et al., 1981](#)). [Weber et al. \(2011\)](#), for instance, interpreted a low velocity region inferred from their analysis of seismological data on the Moon by partial melting. However, a relatively large amount of melt ($\sim 1\%$ or more) is needed for such a model, and retaining a substantial amount of melt in the gravity field is difficult due to the efficient compaction especially in an environment where melt is not produced continuously (e.g., [Hernlund and Jellinek, 2010](#); [Karato, in press](#); [Ribe, 1985](#)). Consequently, I conclude that a partial melt model is unlikely to explain the high electrical conductivity and low tidal Q .

3.4. Frequency dependence of tidal Q

[Williams et al. \(2001\)](#) reported that tidal Q associated with Moon–Earth tide is smaller than that associated with Moon–Sun tide, implying a negative sign of frequency dependence, $\alpha = -0.19$ in $Q^{-1} \propto \omega^{-\alpha}$ ([Efroimsky, 2012](#) also reported $\alpha = -0.09$). This is different from commonly observed frequency dependence of Q ($\alpha \approx 0.3$) both in laboratory studies (e.g., [Jackson, 2009](#)) and in seismological studies (e.g., [Anderson and Minster, 1979](#); [Shito et al., 2004](#)). Two models were proposed to explain this observation.

One is to assume that this represents the edge of the absorption band at the tidal frequency ([Nimmo et al., 2012](#)). In this model, it is considered that there is a low cut-off frequency for the absorption band model above the frequency corresponding to the annual tide ($\sim 10^{-7}$ Hz). However, the validity of this model is dubious because the low cut-off frequency has never been observed in the high temperature experiments of anelasticity in olivine (e.g., [Jackson and Faul, 2010](#)). Rather, at low frequencies, the frequency dependence of Q becomes stronger (larger α in $Q^{-1} \propto \omega^{-\alpha}$) suggesting the gradual transition to the Maxwell behavior.

Another explanation is to invoke the influence of the frequency dependence of the Love number, k_2 . [Efroimsky \(2012\)](#) noted that tidal Q is observed as a combination of $k_2 Q^{-1}$, the frequency dependence of tidal Q (measured as $k_2 Q^{-1}$) is different from that of the intrinsic anelasticity of a material, Q^{-1} . As a consequence, there is a peak in $k_2 Q^{-1}$ at a certain frequency defined by $\omega_t \approx \frac{8\pi G \rho^2 R^2}{57\eta}$ (M is the mass of the Moon, G is the gravity constant, R is the radius of the Moon and ρ is the density of the Moon; [Efroimsky, 2012](#)) across which the frequency dependence changes its sign. If this transition frequency were between monthly and annual tidal frequencies, then $\eta \approx 10^{16}$ Pas. This is much smaller than the viscosity of Earth's asthenosphere ($\sim 10^{18}$ – 10^{20} Pas; e.g., [Nakada and Lambeck, 1989](#); [Pollitz et al., 1998](#)). In fact, [Nakada and Karato \(2012\)](#) showed that the Love number for Earth changes with frequency by only less than $\sim 10\%$ for the frequency range from seismic to tidal frequency. Because the Moon likely has higher viscosity than Earth, I assume that the variation of k_2 with frequency in the Moon is similarly small. Furthermore, tidal Q depends not only on Q in the hot soft

regions but also depends on Q in the mid-mantle where viscosity is much higher (see Fig. 3). Therefore I conclude that this explanation is unlikely valid.

An alternative, and more physically plausible explanation is that the difference in Q between two tidal deformations is due to the difference in the stress (strain) level. Anelastic energy loss is linear when deformation occurs at low stress (low strain). However, when deformation occurs at high stress (and high temperature), anelasticity becomes non-linear, leading to higher energy dissipation at higher stress (strain) (e.g., Karato and Spetzler, 1990; Lakki et al., 1998). The critical strain in most oxides is $\sim 10^{-6}$. The average strain for the Moon–Earth tide is $\sim 2 \times 10^{-6}$, while tidal strain associated with the Moon–Sun tide is $\sim 10^{-8}$ (Murray and Dermott, 1999). It is therefore possible that non-linear anelasticity is a part of the cause of this “frequency” dependence. If this interpretation were correct, it would imply that the Q value for the monthly tide is somewhat under-estimated. However, the strain associated with the Moon–Sun tide is small and anelasticity is likely linear.

3.5. Implications for the formation processes of the Moon

How could the Moon have acquired a substantial amount of water if the Moon were formed by a giant impact? High temperature environment was likely produced by the giant impact (Canup, 2004b), and the degassing in a growing Moon with extensive magma ocean likely led to the depletion of volatile elements from the shallow regions. However, the degree of volatile loss caused by a giant impact itself may be limited: Using the plausible range of temperature, mass and the dimension of a Moon-forming disk, one can conclude that a majority of materials in the Moon-forming disk (or nebula) is gravitationally bound. Therefore the key steps for volatile loss are the condensation and subsequent accretion. If condensed materials do not have much water, then the Moon will be dry.

The analysis of orbital evolution suggests that the Moon was formed close to Earth ($\sim 2.5\text{--}3.0R_E$ (R_E : Earth radius)) and the size of the disk is likely several times R_E (e.g., Canup, 2004a; Stevenson, 1987). If this is the case, then the hot gaseous materials ejected by a giant impact will have relatively high pressure (10^{-2} MPa) (Fig. 6) (see also Ward, 2012 who also studied the vertical structure of the disk) compared to the pressures in the typical regions of the solar nebula ($\sim 10^{-5}\text{--}10^{-3}$ MPa at ~ 1 AU; Cameron and Pine, 1973). Condensation under such a condition should produce a liquid phase rather than a solid phase (Mysen and Kushiro, 1988; Yoneda and Grossman, 1995). As shown in Fig. 7 liquids can dissolve much larger amount of water than solids. However, when liquids solidify, they will lose most of volatiles. Therefore, the necessary condition for a growing planet to maintain a substantial amount of water is that the accretion timescale is faster than or comparable to the cooling timescale: under these conditions, before a majority of water is lost by solidification, a planet can be formed mostly from liquids that can contain a substantial amount of water. The cooling timescale of such a disk is estimated to be $\sim 10\text{--}100$ years at $T \sim 1500$ K (e.g., Canup, 2004a) while the timescale of accretion is on the order of ~ 1 year or less (Ida et al., 1997). If the Moon formation occurs mostly from liquid, it will take ~ 100 years (Salmon and Canup, 2012), but this timescale is not much longer than the cooling timescale, so that a significant amount of liquids should be involved in accretion.

The water content in the liquids depends on the water fugacity. The water fugacity in the Moon-forming disk in turn depends on the total water content and the gas pressure and is highly uncertain (e.g., Ward, 2012). However, it is seen from Fig. 7 that in order to have 0.01–0.1 wt% water in the molten basalt, one only needs the water fugacity of $\sim 10^{-4}$ MPa or higher. Translating this into

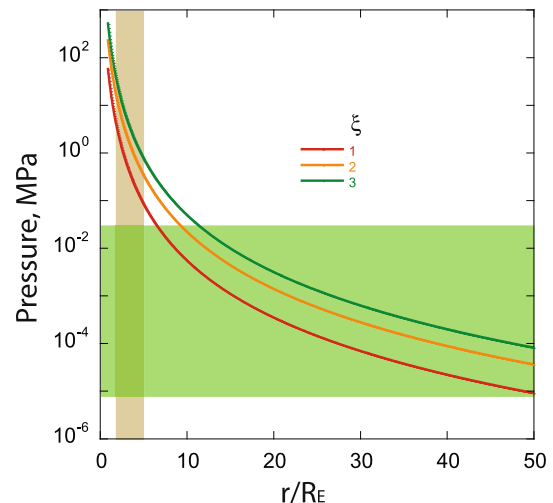


Fig. 6. Pressure in the Moon-forming disk (average pressure) as a function of its size and total mass. For simplicity, I used an equation for a spherical homogeneous disk, $P = \frac{3GM^2}{8\pi r^4}$ where G is the gravity constant, M is the mass of the disk (ξ is the mass of the disk with a unit of the lunar mass) and r is the radius of the disk (in more detail, the pressure varies with the vertical distance, Ward, 2012). The Moon is considered to have been formed at/or near the Roche limit ($\sim 2.7R_E$; R_E : Earth's radius) (regions shown by an orange band). The size of the disk is about a few times the Roche limit (Canup, 2004b). Similar results are obtained by a more elaborated calculation by Ward (2012). The pressure range shown by a green band corresponds to the critical pressure above which gas condenses to liquid phase that depends on the composition (Mysen and Kushiro, 1988; Yoneda and Grossman, 1995). (For interpretation of the references to color in this figure, the reader is referred to the web version of this article.)

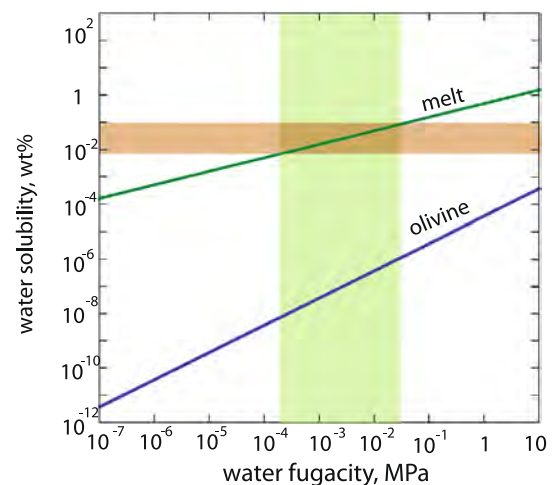


Fig. 7. The water solubility in molten basalt and olivine as a function of water fugacity. Molten basalt has considerably higher water solubility than olivine (based on data by Bolfan-Casanova, 2005; Silver and Stolper, 1985). The water fugacity in a gas-rich disk is essentially the molar fraction of water times the total pressure.

the fraction of water in the disk, it will be $\sim 0.01\text{--}0.1\%$ or higher for the total pressure of $\sim 0.1\text{--}1$ MPa. $\sim 0.01\text{--}0.1\%$ of water corresponds to $\sim 1\text{--}10$ time of the current ocean mass (for Earth), and I consider that this amount of water is not unreasonable in the Moon-forming disk (e.g., Karato, 2011).

In this model, relatively high water content of the lunar interior is a consequence of the small size of a disk (nebula) from which the Moon was formed that caused relatively high pressure and quick accretion. A substantial amount of water retained in the Moon changes many physical properties including tidal Q that has an important influence on the orbital and thermal evolution of the Earth–Moon system.

4. Concluding remarks

I showed that good constraints on water content and temperature in the lunar mantle can be obtained from the electrical conductivity and tidal Q of the Moon. I conclude that the lunar mantle is colder than Earth's mantle but has water content similar to the asthenosphere of Earth.

The present study also suggests some areas where further studies are important. (i) The electrical conductivity-depth profile was inferred from a limited data set using the transfer function approach (comparing the magnetic field strength along different directions). Similar studies using alternative approaches such as magnetotelluric method would also be useful particularly at different locations (these studies will also reveal the lateral variation) (Grimm and Delory, 2012). (ii) Similarly, more observations on Q would be useful. Seismological observations conducted during the Apollo mission are limited (Garcia et al., 2011; Nakamura et al., 1982). Further studies on Q in the deep mantle will be critical. (iii) In the mineral physics side, experimental studies on Q are still limited. Two issues are important in placing better constraints on water content. First, the water effects on attenuation need to be quantified. Second, the transition strain from linear to non-linear attenuation needs to be determined experimentally.

The present study provides a few new insights into the formation and early evolution of the Moon (and other planets, satellites). In most of previous studies on the chemistry of terrestrial planets, condensation of solid phases from the solar nebula was considered (e.g., Grossman and Larimer, 1974; Lewis, 1972). In the formation processes of the Moon, however, the pressure of the “nebula” (or a “disk”) is high and consequently, the first condensed materials are mostly liquid phases. The role of liquid phases during planetary formation should be studied in more detail.

Acknowledgements

I thank Jerry Schubert and Michael Efroimsky for the discussions on tidal dissipation, Robin Canup and Kaveh Pahlevan for the discussion on the lunar accretion models, Amir Khan for the structure of the Moon and Robert Farla for the discussion on anelasticity. Michael Efroimsky and Robert Grimm and another anonymous reviewer provided thoughtful reviews to improve this paper. Francis Nimmo, Larry Grossman and Lindy Elkins-Tanton provided helpful comments. Jun Yi helped numerical calculations on Al_2O_3 partitioning.

References

- Aizawa, Y., Barnhoorn, A., Faul, U.H., Fitz Gerald, J.D., Jackson, I., Kovács, I., 2008. Seismic properties of Anita Bay dunite: An exploratory study of the influence of water. *J. Petrol.* 49, 841–855.
- Anderson, D.L., Minster, J.B., 1979. The frequency dependence of Q in the Earth and implications for mantle rheology and Chandler wobble. *Geophys. J. R. Astron. Soc.* 58, 431–440.
- Bevington, P.R., Robinson, D.K., 2003. *Data Reduction and Error Analysis for the Physical Sciences*. McGraw-Hill, New York.
- Bolfan-Casanova, N., 2005. Water in the Earth's mantle. *Mineral. Mag.* 69, 229–257.
- Boyce, J.W., Liu, Y., Rossman, G.R., Guan, Y., Eiler, J.M., Stolper, E.M., Taylor, L.A., 2010. Lunar apatite with terrestrial volatile abundances. *Nature* 466, 466–470.
- Cameron, A.G.W., Pine, M.R., 1973. Numerical models of the primitive solar nebula. *Icarus* 18, 377–406.
- Canup, R.M., 2004a. Dynamics of lunar formation. *Annu. Rev. Astron. Astrophys.* 42, 441–475.
- Canup, R.M., 2004b. Simulation of a late lunar-forming impact. *Icarus* 168, 433–456.
- Dai, L., Karato, S., 2009a. Electrical conductivity of orthopyroxene: Implications for the water content of the asthenosphere. *Proc. Jpn. Acad.* 85, 466–475.
- Dai, L., Karato, S., 2009b. Electrical conductivity of pyrope-rich garnet at high temperature and pressure. *Phys. Earth Planet. Inter.* 176, 83–88.
- Dai, L., Karato, S., 2009c. Electrical conductivity of wadsleyite under high pressures and temperatures. *Earth Planet. Sci. Lett.* 287, 277–283.
- Dixon, J.E., Leist, L., Langmuir, J., Schilling, J.G., 2002. Recycled dehydrated lithosphere observed in plume-influenced mid-ocean-ridge basalt. *Nature* 420, 385–389.
- Dziewonski, A.M., Anderson, D.L., 1981. Preliminary reference Earth model. *Phys. Earth Planet. Inter.* 25, 297–356.
- Efroimsky, M., 2012. Tidal dissipation compared to seismic dissipation: in small bodies, Earths, and super-Earths. *Astrophys. J.* 746, 150–170.
- Elkins-Tanton, L., Burgess, S., Yin, Q.-Z., 2011. Lunar magma ocean: Reconciling the solidification process with lunar petrology and chronology. *Earth Planet. Sci. Lett.* 304, 326–336.
- Elkins-Tanton, L., Grove, T.L., 2011. Water (hydrogen) in the lunar mantle: Results from petrology and magma ocean modeling. *Earth Planet. Sci. Lett.* 307, 173–179.
- Farla, R., Jackson, I., Fitz Gerald, J.D., Faul, U.H., Zimmerman, M.E., 2012. Dislocation damping and anisotropic seismic wave attenuation in Earth's upper mantle. *Science* 336, 332–335.
- Faul, U.H., Jackson, I., 2005. The seismological signature of temperature and grain size variations in the upper mantle. *Earth Planet. Sci. Lett.* 234, 119–134.
- Frost, D.J., McCammon, C., 2008. The redox state of Earth's mantle. *Annu. Rev. Earth Planet. Sci.* 36, 389–420.
- Garcia, R.F., Gagnepain-Beyneix, J., Chevrot, S., Lognonné, P., 2011. Very preliminary reference Moon model. *Phys. Earth Planet. Inter.* 188, 96–113.
- Greenwood, J.P., Itoh, S., Sakamoto, N., Warren, P., Taylor, L.A., Yurimoto, H., 2011. Hydrogen isotope ratios in lunar rocks indicate delivery of cometary water to the Moon. *Nat. Geosci.* 4, 79–82.
- Grimm, R.E., 2013. Geophysical constraints on the lunar Procellarum KREEP Terrane. *J. Geophys. Res.* 118, <http://dx.doi.org/10.1029/2012JE004114>.
- Grimm, R.E., Delory, G.T., 2012. Next-generation electromagnetic sounding of the Moon. *Adv. Space Res.* 50, 1687–1701.
- Grossman, L., Larimer, J.W., 1974. Early chemical history of the solar system. *Rev. Geophys. Space Phys.* 12, 71–101.
- Hauri, E.H., Weinreich, T., Saal, A.E., Rutherford, M.C., Van Orman, J.A., 2011. High pre-eruptive water contents preserved in lunar melt inclusions. *Science* 333, 213–215.
- Hernlund, J.W., Jellinek, A.M., 2010. Dynamics and structure of a stirred partially molten ultralow-velocity zone. *Earth Planet. Sci. Lett.* 296, 1–8.
- Hirsch, L.M., Shankland, T.J., 1993. Quantitative olivine-defect chemical model: insights on electrical conduction, diffusion and the role of Fe content. *Geophys. J. Int.* 114, 21–35.
- Hirschmann, M.M., 2006. Water, melting, and the deep Earth H_2O cycle. *Annu. Rev. Earth Planet. Sci.* 34, 629–653.
- Hood, L.L., Herbert, F., Sonett, C.P., 1982a. The deep lunar electrical conductivity profile: Structural and thermal inferences. *J. Geophys. Res.* 87, 5311–5326.
- Hood, L.L., Herbert, F., Sonett, C.P., 1982b. Further efforts to limit lunar internal temperatures from electrical conductivity determinations. In: *Proceedings of the Thirteenth Lunar and Planetary Science Conference, Part 1*, pp. A109–A116.
- Huebner, J.S., Wiggins, L.B., Duba, A.G., 1979. Electrical conductivity of pyroxene which contains trivalent cations: Laboratory measurements and the lunar temperature profiles. *J. Geophys. Res.* 84, 4652–4656.
- Ida, S., Canup, R.M., Stewart, G.R., 1997. Lunar accretion from an impact-generated disk. *Nature* 389, 353–357.
- Jackson, I., 2009. Properties of rocks and minerals—physical origins of anelasticity and attenuation in rock. In: Schubert, G. (Ed.), *Treatise on Geophysics*. Elsevier, Amsterdam, pp. 493–525.
- Jackson, I., Faul, U.H., 2010. Grain-size-sensitive viscoelastic relaxation in olivine: Towards a robust laboratory-based model for seismological application. *Phys. Earth Planet. Inter.* 183, 151–163.
- Karato, S., 1984. Grain-size distribution and rheology of the upper mantle. *Tectonophysics* 104, 155–176.
- Karato, S., 1998. A dislocation model of seismic wave attenuation and velocity dispersion and microcreep of the solid Earth: Harold Jeffreys and the rheology of the solid Earth. *Pure Appl. Geophys.* 153, 239–256.
- Karato, S., 2006. Remote sensing of hydrogen in Earth's mantle. In: Keppler, H., Smyth, J.R. (Eds.), *Water in Nominally Anhydrous Minerals*. Mineralogical Society of America, Washington, DC, pp. 343–375.
- Karato, S., 2008. *Deformation of Earth Materials: Introduction to the Rheology of the Solid Earth*. Cambridge University Press, Cambridge.
- Karato, S., 2010. Rheology of the deep upper mantle and its implications for the preservation of the continental roots: A review. *Tectonophysics* 481, 82–98.
- Karato, S., 2011. Water distribution across the mantle transition zone and its implications for global material circulation. *Earth Planet. Sci. Lett.* 301, 413–423.
- Karato, S., in press. Does partial melting explain geophysical anomalies?. *Phys. Earth Planet. Inter.*
- Karato, S., 2013. Theory of isotope diffusion in a material with multiple-species and its implications for hydrogen-enhanced electrical conductivity in olivine. *Phys. Earth Planet. Inter.* 219, 49–54.
- Karato, S., Jung, H., 2003. Effects of pressure on high-temperature dislocation creep in olivine polycrystals. *Philos. Mag.* A 83, 401–414.
- Karato, S., Spetzler, H.A., 1990. Defect microdynamics in minerals and solid state mechanisms of seismic wave attenuation and velocity dispersion in the mantle. *Rev. Geophys.* 28, 399–421.

- Karato, S., Toriumi, M., Fujii, T., 1980. Dynamic recrystallization of olivine single crystals during high temperature creep. *Geophys. Res. Lett.* 7, 649–652.
- Karato, S., Wang, D., 2013. Electrical conductivity of minerals and rocks. In: Karato, S. (Ed.), *Physics and Chemistry of the Deep Earth*. Wiley–Blackwell, New York, pp. 145–182.
- Katayama, I., Karato, S., 2008. Effects of water and iron content on the rheological contrast between garnet and olivine. *Phys. Earth Planet. Inter.* 166, 59–66.
- Khan, A., Connolly, J.A.D., Maclennan, J., Mosegaard, K., 2007. Joint inversion of seismic and gravity data for lunar composition and thermal state. *Geophys. J. Int.* 168, 243–258.
- Khan, A., Connolly, J.A.D., Olsen, N., Mosegaard, K., 2006. Constraining the composition and thermal state of the moon from an inversion of electromagnetic lunar day-side transfer functions. *Earth Planet. Sci. Lett.* 248, 579–598.
- Konopliv, A.S., Asmar, S.W., Carranza, E., Sjogren, W.L., Yuan, D.N., 2001. Recent gravity models as a result of the Lunar Prospector mission. *Icarus* 150, 1–18.
- Kuskov, O.L., Kronrod, V.A., 1998. Constitution of the Moon: 5. Constraints on composition, density, temperature, and radius of a core. *Phys. Earth Planet. Inter.* 107, 285–306.
- Lakki, A., Schaller, R., Carry, C., Benoit, W., 1998. High temperature anelastic and viscoelastic deformation of fine-grained MgO-doped Al₂O₃. *Acta Mater.* 46, 689–700.
- Lambeck, K., Pullan, S., 1980. Inferences on the lunar temperature from gravity, stress and flow laws. *Phys. Earth Planet. Inter.* 22, 12–28.
- Lewis, J.S., 1972. Metal/silicate fractionation in the Solar System. *Earth Planet. Sci. Lett.* 15, 286–290.
- McCarthy, C., Takei, Y., Hiraga, T., 2011. Experimental study of attenuation and dispersion over a broad frequency range: 2. The universal scaling of polycrystalline materials. *J. Geophys. Res.* 116, <http://dx.doi.org/10.1029/2011JB008384>.
- McKenzie, D., Bickle, M.J., 1988. The volume and composition of melt generated by extension of the lithosphere. *J. Petrol.* 29, 625–679.
- Mei, S., Kohlstedt, D.L., 2000a. Influence of water on plastic deformation of olivine aggregates, 1. Diffusion creep regime. *J. Geophys. Res.* 105, 21457–21469.
- Mei, S., Kohlstedt, D.L., 2000b. Influence of water on plastic deformation of olivine aggregates, 2. Dislocation creep regime. *J. Geophys. Res.* 105, 21471–21481.
- Murray, C.D., Dermott, S.F., 1999. *Solar System Dynamics*. Cambridge University Press, Cambridge.
- Mysen, B.O., Kushiro, I., 1988. Condensation, evaporation, melting, and crystallization in the primitive solar nebula: Experimental data in the system MgO–SiO₂–H₂ to 10^{−9} bar and 1870 °C with variable oxygen fugacity. *Am. Mineral.* 73, 1–19.
- Nakada, M., Karato, S., 2012. Low viscosity of the bottom of the Earth's mantle inferred from the analysis of Chandler wobble and tidal deformation. *Phys. Earth Planet. Inter.* 192/193, 68–80.
- Nakada, M., Lambeck, K., 1989. Late Pleistocene and Holocene sea-level change in the Australian region and mantle rheology. *Geophys. J. Int.* 96, 497–517.
- Nakamura, Y., Koyama, J., 1982. Seismic *Q* of the lunar upper mantle. *J. Geophys. Res.* 87, 4855–4861.
- Nakamura, Y., Latham, G.V., Dorman, H.J., 1982. Apollo lunar seismic experiment—Final summary. *J. Geophys. Res.* 87, A117–A123.
- Nimmo, F., Faul, U.H., Garnero, E.J., 2012. Dissipation at tidal and seismic frequencies in a melt-free Moon. *J. Geophys. Res.* 117, <http://dx.doi.org/10.1029/2012JE004160>.
- Nishihara, Y., Shinmei, T., Karato, S., 2006. Grain-growth kinetics in wadsleyite: effects of chemical environment. *Phys. Earth Planet. Inter.* 154, 30–43.
- Peale, S.J., Cassen, P., 1978. Contribution of tidal dissipation to lunar thermal history. *Icarus* 36, 245–269.
- Perkins III, D., Holland, T.J.B., Newton, R.C., 1981. The Al₂O₃ content of enstatite in equilibrium with garnet in the system MgO–Al₂O₃–SiO₂ at 15–40 kbar and 900°–1600 °C. *Contrib. Mineral. Petrol.* 78, 99–109.
- Pollitz, F.F., Bürgmann, R., Romanowicz, B., 1998. Viscosity of oceanic asthenosphere inferred from remote triggering of earthquakes. *Science* 280, 1245–1249.
- Ribe, N.M., 1985. The generation and compaction of partial melts in the Earth's mantle. *Earth Planet. Sci. Lett.* 73, 361–376.
- Ringwood, A.E., 1979. *Origin of the Earth and Moon*. Berlin.
- Saal, A.E., Hauri, E.H., Lo Cascio, M., Van Orman, J.A., Rutherford, M.C., Cooper, R.F., 2008. Volatile content of lunar volcanic glasses and the presence of water in the Moon's interior. *Nature* 454, 192–195.
- Salmon, J., Canup, R.M., 2012. Lunar accretion from a Roche-interior fluid disk. *Astrophys. J.* 760, <http://dx.doi.org/10.1088/0004-637X/760/1/83>.
- Schubert, G., Turcotte, D.L., Olson, P., 2001. *Mantle Convection in the Earth and Planets*. Cambridge University Press, Cambridge.
- Shankland, T.J., O'Connell, R.J., Waff, H.S., 1981. Geophysical constraints on partial melt in the upper mantle. *Rev. Geophys. Space Phys.* 19, 394–406.
- Shito, A., Karato, S., Park, J., 2004. Frequency dependence of *Q* in Earth's upper mantle inferred from continuous spectra of body wave. *Geophys. Res. Lett.* 31, <http://dx.doi.org/10.1029/2004GL019582>.
- Silver, L.A., Stolper, E.M., 1985. A thermodynamic model for hydrous silicate melts. *J. Geol.* 93, 161–178.
- Stevenson, D.J., 1987. Origin of the Moon—The collision hypothesis. *Annu. Rev. Earth Planet. Sci.* 15, 271–315.
- Sundberg, M., Cooper, R.F., 2010. A composite viscoelastic model for incorporating grain boundary sliding and transient diffusion creep: Correlating creep and attenuation responses for materials with a fine grain size. *Philos. Mag.* 90, 2817–2840.
- Toksöz, M.N., 1974. Geophysical data and the interior of the Moon. *Annu. Rev. Earth Planet. Sci.* 2, 151–177.
- Ward, W.R., 2012. On the vertical structure of the protolunar disk. *Astrophys. J.* 744, <http://dx.doi.org/10.1088/0004-637X/744/2/140>.
- Weber, R.C., Lin, P.-Y., Garnero, E.J., Williams, Q., Legnonné, P., 2011. Seismic detection of the lunar core. *Science* 331, 309–312.
- Wiechert, U., Halliday, A.N., Lee, D.-C., Snyder, G.A., 2001. Oxygen isotopes and the Moon-forming giant impact. *Science* 294, 345–348.
- Wieczorek, M.A., Jolliff, B.L., Khan, A., Pritchard, M.E., Weiss, B.P., Williams, J.G., Hood, L.L., Righter, K., Neal, C.R., Shearer, C.K., McCallum, I.S., Tomkins, S., Hawke, B.R., Peterson, C., Gillis, J.J., Bussey, B., 2006. The composition and structure of the lunar interior. *Rev. Mineral. Geochem.* 60, 221–364.
- Williams, J.G., Boggs, D.H., Yoder, C.F., Ratcliff, J.T., Dickey, J.O., 2001. Lunar rotational dissipation in solid body and molten core. *J. Geophys. Res.* 106, 27933–27968.
- Xu, Y., Shankland, T.J., Duba, A.G., 2000. Pressure effect on electrical conductivity of mantle olivine. *Phys. Earth Planet. Inter.* 118, 149–161.
- Yang, Y., Forsyth, D.W., Weeraratne, D.S., 2007. Seismic attenuation near the East Pacific Rise and the origin of the low-velocity zone. *Earth Planet. Sci. Lett.* 258, 260–268.
- Yoneda, S., Grossman, L., 1995. Condensation of CaO–MgO–Al₂O₃–SiO₂ liquids from cosmic gases. *Geochim. Cosmochim. Acta* 59, 3413–3444.
- Yoshino, T., 2010. Laboratory electrical conductivity measurement of mantle minerals. *Surv. Geophys.* 31, 163–206.
- Zhang, J., Dauphas, N., Davis, A.M., Leya, I., Fedkin, A., 2012. The proto-Earth as a significant source of lunar material. *Nat. Geosci.* 5, 251–255.
- Zhao, Y.-H., Zimmerman, M.E., Kohlstedt, D.L., 2009. Effect of iron content on the creep behavior of olivine: 1. Anhydrous conditions. *Earth Planet. Sci. Lett.* 287, 229–240.